Micromechanical modeling of time-dependent transverse failure in composite systems

Mechanics of Time-Dependent Materials **4:** 275–291, 2000.

Micromechanical Modeling of Time-Dependent Transverse Failure in Composite Systems

LEON E. GOVAERT
Dutch Polymer Institute, Eindhoven University of Technology, P.O. Box 513, 5600 MB Eindhoven, The Netherlands

TON PEIJS
Department of Materials, Queen Mary and Westfield College, University of London, Mile End Road, London E1 4NS, U.K.

(Received 1 April 1999; accepted 14 July 2000)

Abstract. The time-dependent failure behaviour of transversely loaded composites is investigated, assuming that fracture is matrix dominated. Since the stress and strain state of the matrix in composite structures is complex, the yield and fracture behaviour of a neat epoxy system is investigated under various multi-axial loading conditions. A good description of the multi-axial yielding behaviour of the matrix material is obtained with the three-dimensional pressure modified Eyring equation. The parameters of this three-dimensional yield expression are implemented into a constitutive model, which has been shown to correctly describe the deformation behaviour of polymers under complex loadings. By means of a micromechanical approach, the matrix dominated transverse strength of a unidirectional composite material was investigated. Numerical simulations show that a failure criterion based on maximum strain provides a good description for the rate-dependent transverse strength of unidirectional glass/epoxy composites. Furthermore, such a strain criterion is also able to describe the durability (creep) of transversely loaded unidirectional composites.

Key words: durability, failure, micromechanics, transverse strength, yielding

1. Introduction

Models for the prediction of strength of composite materials are generally directed to short-term failure using laminate analysis based on classical mechanics, coupled with a common failure theory such as maximum stress or maximum strain concepts (Tsai and Hahn, 1980). The input data for these models is derived from standard tests on unidirectional laminates, normally in accordance with the American Society for Testing and Materials (ASTM) standards, and are typically low strain rate or quasi-static experiments. Subsequently, this data is often used by designers to analyze structures which are subjected to long-term static (creep), dynamic (fatigue) or shock (impact) loadings, which all differ strongly from the standard test conditions.

In the field of polymer physics it is well established that the deformation as well as the failure behaviour of polymers is strongly influenced by the time-scale of the

experiment (Brown, 1986; Ward, 1983; Haward and Young, 1997). It is therefore eminent that composites based on these materials will also display a large influence of the time-scale, especially in off-axis loading situations where the properties are strongly governed by the viscoelastic polymer matrix. With respect to durability this implies that the mere fact that a composite material is loaded well below the critical stress, as determined in a short-term test, will not ensure that the material will sustain this load for an infinite period of time.

One of the most important factors determining the failure behaviour of glassy polymers is yielding and the ability or inability to plastically deform. Unlike metals, the development of plastic deformation will occur in polymers at any stress level. Under the influence of an applied stress the development of plastic deformation will start immediately upon loading, and will proceed at a constant rate that depends strongly on the stress level. In a tensile test, the rate of plastic deformation will gradually increase with increasing stress until it is in balance with the externally applied strain rate and a constant level of stress is reached: the yield stress. With decreasing strain rate, or, equivalently, increasing temperature, this yield stress will decrease (Brown, 1986; Ward, 1983; Haward and Young, 1997).

In the present research the transverse failure behaviour of a glass-fibre/epoxy composite is studied in constant strain rate and creep experiments in three-point bending. The experimental results are subsequently analyzed employing micro-mechanics. To facilitate this analysis the deformation behaviour of the epoxy matrix is investigated in detail. Since previous studies already showed the importance of a multi-axial stress state for the initiation of transverse failure (Asp et al., 1995; De Kok et al., 1993; De Kok, 1995), the yield behaviour of the epoxy matrix is characterized in various multi-axial loading conditions. The experimental data is analyzed using a Pressure-modified Eyring equation (Ward, 1971; Duckett et al., 1978).

With recent developments in three-dimensional constitutive modelling of large strain plasticity in amorphous polymers (Boyce et al., 1988, 1994; Wu and Van der Giessen, 1993; Tervoort et al., 1996, 1998), the numerical simulation of the behaviour of the polymer matrix under complex loading conditions is now well established. In the present work a previously developed constitutive model, the so-called compressible Leonov model (Tervoort et al., 1996, 1998), was employed in the micromechanical finite element simulations. In combination with a maximum strain criterion for the epoxy matrix, it is attempted to describe the rate-dependent strength and creep life-time of a transversally loaded unidirectional glass/epoxy composite.

2. Experimental

2.1. MATERIALS

The experimental part of this study consisted of mechanical tests on pure matrix material and on unidirectional composites. For the matrix material a rather brittle epoxy system of Ciba Geigy (Araldite) was used. This epoxy system is based on diglycidyl ether of bisphenol-A (LY556) with an anhydride curing agent (HY917) and an accelerator (DY070) in the weight ratio of 100:90:1. In this study E-glass fibres (Silenka 0.84-M28) were used as reinforcement material.

Samples for experiments on the neat epoxy where milled from plate material. For the fabrication of these plates, the constituents of the epoxy system were carefully mixed. The matrix material was subsequently poured into a preheated aluminium casting-mould and was cured for 4 hours at 80°C and 8 hours at 140°C. Plates (240 $\times$ 180 mm) were made with a thickness of 2, 4 and 6 mm. As a result of exothermic heating, plates thicker than 6 mm showed signs of degradation and were therefore not considered.

Unidirectional composites were manufactured by filament winding. Fibre strands were impregnated in a heated epoxy bath and wound uniformly on a framework. The impregnated fibres were subsequently placed in a mould and cured in a hot press for 4 hours at 80°C and 8 hours at 140°C. The resulting composite plates had a thickness of 1.25 mm and a fibre-volume fraction of approximately 50%. From these unidirectional laminates transverse three-point bending specimens were cut with a length of 50 mm and a width of 25 mm, as suggested by ASTM D790M-92. The edges of all three-point bending samples were manually finished using SiC polishing paper (up to 4000 FEPA Standard).

2.2. TESTING

The experimental part of this study consisted of mechanical test on pure matrix material and on unidirectional composites. In order to characterize the yield behaviour of the matrix under complex stress fields, various test are needed. In this study the material was studied at strain rates varying over several decades in five different loading geometries: uniaxial extension, uniaxial compression, planar extension, planar compression and simple shear. All experiments were performed at room temperature.

Uniaxial tensile tests were performed on 2-mm-thick dog-bone specimens, according to ASTM D638-91. Uniaxial compression samples were end-loaded and measured 10 $\times$ 6 $\times$ 6 mm. The planar extension samples were dog-bone shaped, with a testing section of 50 mm wide, 10 mm long and 2 mm thick. Due to the high width-to-length ratio the contraction of the material is constrained in the width of the sample, which creates a plane strain condition during the straining of the sample (Whitney and Andrews, 1967). Planar compression tests were performed on dog-bone shaped specimens with a test section measuring 85 $\times$ 20 $\times$ 4 mm. In

the test section the specimens were supported by steel plates to create a plane strain condition. Simple shear tests, according to ASTM D4255-83, were performed on samples with a thickness of 2 mm and a length of 100 mm. The distance between the grips was 10 mm, resulting in an aspect ratio of 10.

To determine the transverse material properties of the unidirectional glass fibre reinforced composites, three-point bending test were performed in accordance with ASTM D790M-92. The strain rate in the outer layers of the samples in the three-point bending test varied from 1.7×10^{-6} to 1.7×10^{-3} s^{-1}. A support length of 32 mm and thickness of 1.25 mm resulted in a span-to-depth ratio of 25. The strain rate and creep experiments were both performed on a Frank 81565 tensile tester.

3. Constitutive Modelling

3.1. The Compressible Leonov Model

In previous work an elasto-viscoplastic constitutive equation for polymer glasses was introduced, the so-called compressible Leonov model (Tervoort et al., 1996, 1998). In this model the Cauchy stress tensor σ is decomposed in a hydrostatic and a deviatoric part, and related to the deformations according to:

$$\sigma = K(J-1)\mathbf{I} + G\tilde{\mathbf{B}}_e^d. \tag{1}$$

In this equation K and G are the bulk modulus and the shear modulus respectively. The relative volume change J and the isochoric elastic left Cauchy–Green deformation tensor $\tilde{\mathbf{B}}_e$, are implicitly given by (Tervoort et al., 1998):

$$\dot{J} = \mathrm{tr}\,(\mathbf{D}), \tag{2}$$

$$\overset{\circ}{\tilde{\mathbf{B}}}_e = (\mathbf{D}^d - \mathbf{D}_p^d)\cdot\tilde{\mathbf{B}}_e + \tilde{\mathbf{B}}_e\cdot(\mathbf{D}^d - \mathbf{D}_p^d). \tag{3}$$

The left-hand side of this equation represents the (objective) Jaumann derivative of the isochoric elastic left Cauchy–Green tensor. The tensor $\mathbf{D}$ denotes the rate of deformation tensor, $\mathbf{D}_p$ the plastic rate of deformation tensor. To complete the constitutive description the plastic deformation rate is expressed in the Cauchy stress by a generalized non-Newtonian flow rule (Bird et al., 1987):

$$\mathbf{D}_p = \frac{\sigma^d}{2\eta(\tau_{\mathrm{eq}})} \quad \text{with} \quad \tau_{\mathrm{eq}} = \sqrt{\frac{1}{2}\mathrm{tr}\,(\sigma^d\cdot\sigma^d)}. \tag{4}$$

The viscosity η depends on the equivalent stress τ_{eq}, according to an Eyring relationship (Tervoort et al., 1998):

$$\eta(\tau_{\mathrm{eq}}) = A\tau_0\frac{\tau_{\mathrm{eq}}/\tau_0}{\sinh(\tau_{\mathrm{eq}}/\tau_0)}. \tag{5}$$

In this equation A is a time constant and τ_0 a characteristic stress, respectively related to the activation energy ΔH and the shear activation volume V according to (Tervoort et al., 1998; Ward, 1983):

$$A = A_0 \exp\left[\frac{\Delta H}{RT}\right]; \quad \tau_0 = \frac{RT}{V}. \tag{6}$$

As this study is performed at constant temperature, A and τ_0 are constants.

3.2. Extension to Pressure-Dependent Yield and Strain Hardening

This section describes the extension of the compressible Leonov model to include both the influence of pressure on the yield stress and the strain hardening effect. In that case the Cauchy stress tensor σ is considered as a parallel assemblage of two distinguishable parts: The driving stress tensor $\mathbf{s}$ and the hardening stress tensor $\mathbf{r}$ respectively:

$$\sigma = \mathbf{s} + \mathbf{r}. \tag{7}$$

The expression for $\mathbf{s}$ is derived from the compressible Leonov model described above (Tervoort et al., 1998):

$$\mathbf{s} = K(J-1)\mathbf{I} + G\tilde{\mathbf{B}}_e^d, \tag{8}$$

where K is the bulk modulus, G is the shear modulus, J is the elastic volume change, and $\tilde{\mathbf{B}}_e$, denotes the isochoric fraction of the elastic left Cauchy–Green tensor. Also in this case, the evolution of $\tilde{\mathbf{B}}_e$, is given by Equation (3). To complete the constitutive description the plastic deformation rate is still expressed in the Cauchy stress tensor by a generalized non-Newtonian flow rule:

$$\mathbf{D}_p = \frac{\mathbf{s}^d}{2\eta(\tau_{\text{eq}}, p)}, \tag{9}$$

where τ_{eq} and p are parameters to be defined in the following. The viscosity η is derived assuming pressure modified Eyring flow (Ward, 1971; Duckett et al., 1978):

$$\dot{\gamma}_{\text{eq}} = \frac{1}{A}\sinh\left[\frac{\tau_{\text{eq}}}{\tau_0}\right]\exp\left[-\frac{\mu P}{\tau_0}\right], \tag{10}$$

where $\dot{\gamma}_{\text{eq}}$ is the equivalent shear rate, τ_{eq} is the equivalent shear stress and p is the hydrostatic pressure, according to:

$$\dot{\gamma}_{\text{eq}} = \sqrt{\text{tr}\,(\mathbf{D}_p \cdot \mathbf{D}_p)}, \tag{11}$$

$$\tau_{\text{eq}} = \sqrt{\frac{1}{2}\text{tr}\,(\mathbf{s}^d \cdot \mathbf{s}^d)}, \tag{12}$$

$$p = -\frac{1}{3}\mathrm{tr}\,(\mathbf{s}). \tag{13}$$

In this case, the viscosity function η can be expressed as

$$\eta(\tau_{\mathrm{eq}}, p) = A\tau_0 \exp\left(\frac{\mu p}{\tau_0}\right) \frac{\tau_{\mathrm{eq}}/\tau_0}{\sinh(\tau_{\mathrm{eq}}/\tau_0)}, \tag{14}$$

where A is a time constant, τ_0 a characteristic stress. The parameter μ is a pressure coefficient, related to the shear activation volume V and the pressure activation volume Ω according to:

$$\mu = \frac{\Omega}{V}. \tag{15}$$

The hardening behaviour of the material is described by the hardening stress tensor **r**. In studies on the deformation behaviour of glassy polymers, it is common practice to model the hardening behaviour as a generalized rubber elastic spring with finite extensibility, like the so-called three-chain and eight-chain models of Arruda and Boyce (1993), or the full chain model of Wu and Van der Giessen (1993). On the other hand, Haward (1993) applied network models employing Gaussian chain statistics (leading to a neo-Hookean strain hardening response) to experimental uniaxial stress-strain curves, and concluded that some amorphous and most semi-crystalline polymers obeyed this formulation. Generalization to three dimensions, in the assumption that the network is incompressible, leads to the following neo-Hookean relationship for the hardening stress tensor **r**:

$$\mathbf{r} = G_R \tilde{\mathbf{B}}^d \tag{16}$$

with G_R the strain hardening modulus (assumed temperature independent). Contrary to Boyce et al. (1988) the hardening stress is not related to the plastic deformation but to the total deformation. This adaptation is introduced because in the present approach both elastic and plastic deformations are assumed to decrease the configurational entropy of the polymer.

3.3. Material Characterization

3.3.1. *Elastic Parameters*

The elastic modulus E and the Poisson's ratio ν of the matrix material were 3200 MPa and 0.37 respectively, as determined in a tensile experiment. The elastic properties of the glass fiber were assumed $E = 70$ GPa and $\nu = 0.22$.

3.3.2. *Yield Parameters*

The results of the uniaxial extension, planar extension, uniaxial compression, planar compression and simple shear test, all performed at a temperature of 22°C,

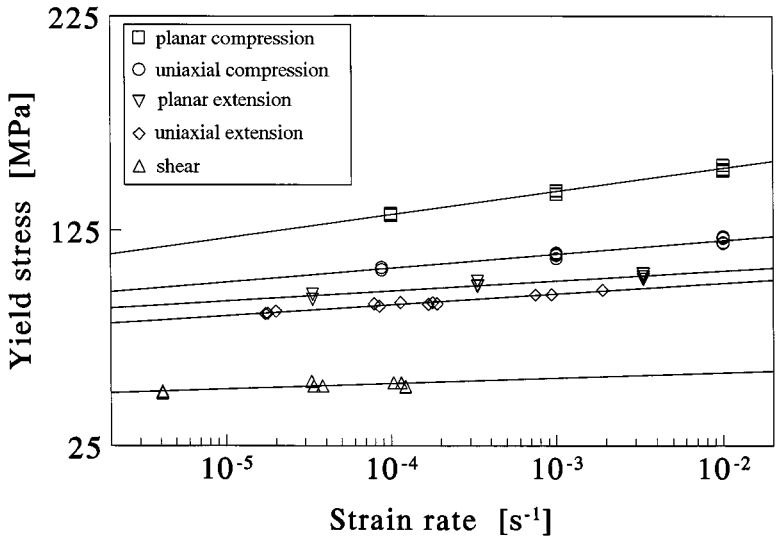

Figure 1. The true yield stress *versus* true strain rate for the various test conditions. The drawn lines are visual fits.

Table I. Values of the yield parameters for the epoxy matrix (see Equation (10)).

A (s)	τ_0 (MPa)	μ
8.2×10^{20}	1.426	0.126

are presented in Figure 1. In this figure the true stress, obtained at the yield point, is plotted *versus* the applied strain rate. In uniaxial extension the increase of the yield stress is approximately 5 MPa/decade. In reverse this implies that an increase of the stress with 5 MPa will result in an increase of the plastic deformation rate by a factor of 10.

The results of the experiments are converted into the equivalent shear stress and strain rate, which are presented in Figure 2. This figure clearly demonstrates the pressure-dependence of the material since the results of the different loading geometries are not the same. This is the influence of the parameter μ, which increases the equivalent shear stress at the yield point with increasing hydrostatic pressure. In the absence of this pressure dependence all loading geometries would yield the same plot of τ_{eq} *versus* $\dot{\gamma}_{eq}$.

The values of the parameters A, τ_0, and μ were calculated by a fitting procedure on the data of the uniaxial extension and the uniaxial compression test. The parameters obtained are given in Table I. The solid lines in Figure 2 are predictions employing Equation (10) with the parameters listed in Table I. It is clearly shown

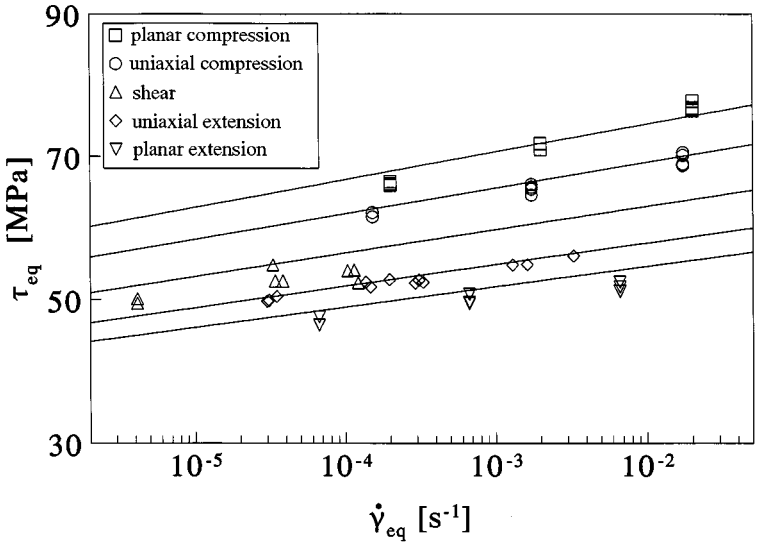

Figure 2. The equivalent shear stress *versus* equivalent shear rate for the various test conditions. The solid lines are predictions according to Equation (10) with the parameters listed in Table I.

that the model predictions with the pressure-modified Eyring equation are in good agreement with the experimental data.

3.3.3. *Hardening Modulus*

The hardening parameter G_R is, in the present study, determined in a uniaxial compression test. Figure 3 shows the result of a uniaxial compression experiment at a strain rate of 10^{-4} s^{-1}. In this figure the axial true stress a is plotted as a function of the strain measure $\lambda^2 - \lambda^{-1}$. This strain measure is, in a uniaxial compression (or tensile) test, the component of the deviatoric isochoric left Cauchy green deformation tensor $\tilde{\mathbf{B}}^d$ in load direction. According to the neo-Hookean approach, the compression curve should display a constant slope after yield. As shown in Figure 3, this assumption is valid up to compressive strains of approximately 15%. At higher strain levels the slope is increasing, indicating a possible influence of the limited extensibility of the epoxy network. In the present work, the neo-Hookean approach was chosen, since it was readily available in the finite element code. From Figure 3, the value of the strain hardening modulus G_R was determined to be 10.5 MPa.

4. Micromechanical Analysis of Composite Materials

Micromechanics is an effective tool that can be employed to estimate the mechanical or physical properties of a composite material on the basis of the properties of its constituents and their microstructural ordering. To analyze a microstructure by

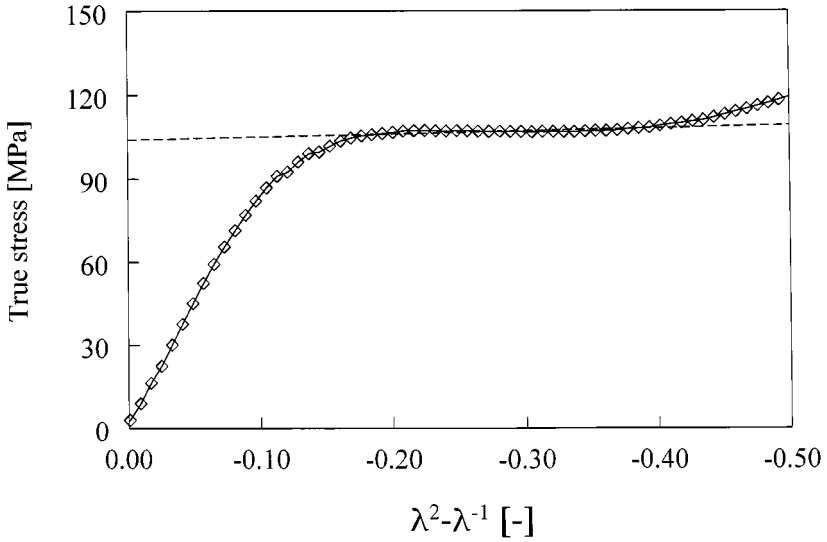

Figure 3. True stress *versus* $\lambda^2 - \lambda^{-1}$ for a compression test on the neat epoxy matrix at a strain rate of 10^{-4} s^{-1}. The dashed line indicates the neo-Hookean strain hardening behaviour with a strain hardening modulus of 10.5 MPa.

a micromechanical finite element simulation, there are basically two requirements: (1) the choice of an appropriate constitutive law, that is able to describe the different features of the deformation behaviour correctly, and (2) the definition of a representative volume element that accounts for the microstructural arrangement of the components. In our case, where its attempted to analyze (time-dependent) failure phenomena, an additional failure criterion needs to be chosen and quantified.

4.1. Finite Element Model

In the case of transversely loaded unidirectional composites, the microstructure is characterized by a random arrangement of fibres in a polymer matrix. Since a detailed geometrical model of this microstructure would lead to excessive computing time, especially in the case of time-dependent behaviour, the topography is usually simplified by assuming a more regular stacking of the fibres. A successful simplification is to assume that the fibres are stacked regularly in a hexagonal array (De Kok, 1995), from which the repeating unit is shown in Figure 4a. Due to symmetry only a quarter of this repeating unit needs to be modelled (see Figure 4b), which leads to a decrease in elements and thus simulation time. The finite element mesh has been created with the pre-processor Mentat 120 and is shown in Figure 5. The mesh represents a fibre-volume fraction of 50% and consists of 880 generalized plane strain quadrilateral elements. The influence of element size on the results of the simulation was eliminated by sufficient refining of the mesh, especially in the matrix area near the fibre/matrix interface.

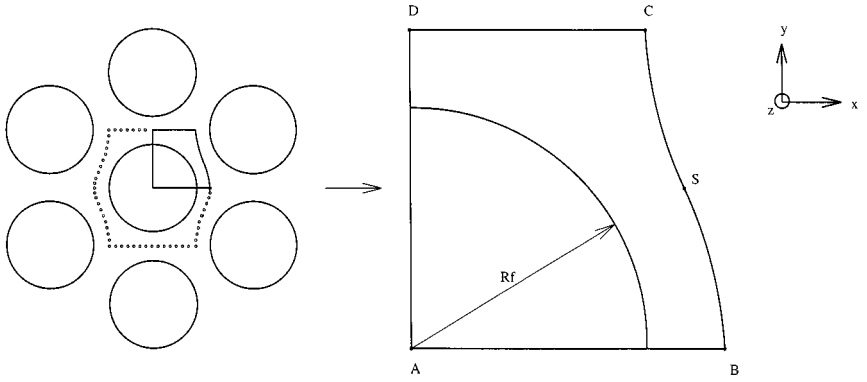

Figure 4. (a) Representation of the hexagonal stacking pattern. (b) Due to symmetry only a quarter of the repeating unit has to be modeled. R_f is the radius of the fibre.

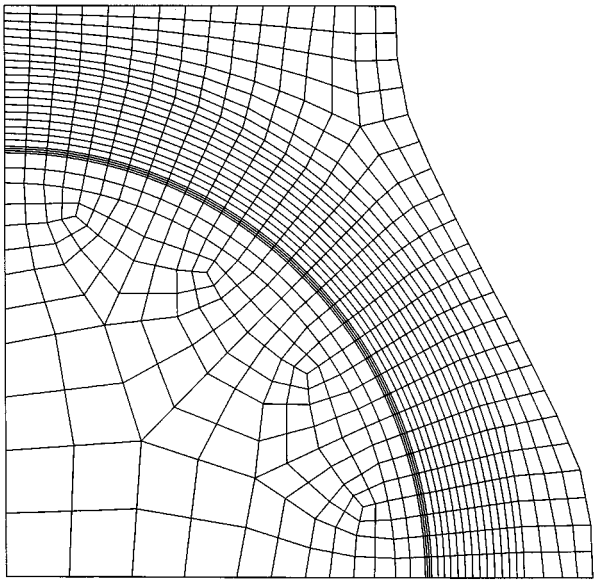

Figure 5. The finite element mesh used in this study.

The corresponding boundary conditions for the quarter of the repeating unit are indicated in Figure 4b. The displacement in y-direction is zero on side AB. The displacement in x-direction is zero on side AD. The displacement in y-direction is constant on side DC. Therefore the nodes on side DC are tied in y-direction. In the numerical simulations the displacements and forces are applied on this side. On side BC an anti-symmetrical curve is chosen through midpoint S. This curve

has to remain anti-symmetrical throughout the simulation. Therefore, points on the curve equidistant from midpoint S should have an equal but opposite displacement in x and y-directions in comparison with the displacement of the midpoint.

In the simulations the macroscopic strain is obtained by dividing the displacement of the line DC in y-direction by the initial length of the line AD. The macroscopic stress is obtained by dividing the total reaction force on side DC by its cross-sectional area.

4.2. Failure Criterion: A Hybrid Experimental/Numerical Approach

With the geometrical assumptions and the choice of the constitutive behaviour, we are now able to numerically simulate the mechanical response of unidirectional composites in transverse loading. However, since there are no restrictions to the deformation within the constitutive model, an additional failure criterion for the matrix material has to be defined. For the prediction of failure at a certain strain rate or under the influence of a statically applied *global* stress (creep) this criterion is employed to detect local failure in the representative volume element during a simulated loading sequence.

In this study a critical strain criterion was chosen, more specifically a critical value for the equivalent shear strain, being a second invariant of the total strain tensor:

$$\gamma_{\text{eq}} = \frac{2}{3}\sqrt{[(\varepsilon_1 - \varepsilon_2)^2 + (\varepsilon_2 - \varepsilon_3)^2 + (\varepsilon_3 - \varepsilon_1)^2]}. \tag{17}$$

In traditional micromechanics the critical value of the failure criterion is based on experiments on the neat matrix material. This approach was successfully employed in parametric studies, e.g. trends of the influence of matrix yield stress, fibre-volume fraction, fibre/matrix adhesion or interphase properties (De Kok, 1995). However, it can easily be anticipated that this method will not lead to the quantitative prediction of time-dependent transverse failure aimed for in this study. The reason for this anticipated discrepancy is that the present micromechanical analysis is based on a hexagonal stacking pattern instead of the random stacking pattern that is characteristic for a real composite. In the actual case local variations in fibre-volume fraction, flaws, and voids will strongly influence the local stress situation in the matrix, and global fracture will be initiated from these imperfections. With respect to the aim of this study being lifetime prediction of composite materials, this is especially the case, since relative small changes in the (local) stress level will lead to large changes in local plastic deformation rates and thus strong variations in lifetime predictions. In the micromechanical simulations, based on a regular stacking pattern, the influence of imperfections is omitted and consequently the strength and lifetime of the composite will be overestimated when based on the true matrix strength. A possible solution to this problem would be to use a more realistic geometrical model, e.g. a random stacking pattern. However, as a

result of this complex geometry the computing time, required for the numerical simulations, would increase strongly. This is especially the case when a nonlinear, time-dependent constitutive equation like the compressible Leonov model is employed.

As an alternative route, we introduce a hybrid experimental/numerical technique. In this approach the critical value of the failure criterion is 'calibrated' on a reference experiment. In this technique a reference experiment is chosen, in our case a constant strain rate experiment at a rate of 1.7×10^{-4} s^{-1}, and the mean value of the tensile strength is determined experimentally. Subsequently a micromechanical simulation of the experiment is performed up to the point where the applied global stress in the simulation equals the experimentally obtained tensile strength. At this stress level the local strain distribution is evaluated and the critical value for the equivalent shear strain γ_{eq} is set equal to the local maximum of γ_{eq}.

It should be noted once more that the critical value for the equivalent shear strain obtained by this hybrid experimental/numerical technique is *not* equal to the characteristic failure criterion of the neat epoxy. In our approach the composite is regarded as a homogeneously stacked material and therefore the influence of all the imperfections mentioned above are incorporated in a single criterion: the obtained value of γ_{eq}. Unfortunately, this implies that the critical value obtained for the criterion is to be regarded as characteristic for the material used in this study, and is very likely to change when material parameters like fibre-volume fraction is varied. On the other hand, this procedure quantifies the effect of imperfections, and enables us to give a quantitative prediction of time-dependent transverse failure in this material.

5. Model Validation

5.1. Rate-Dependent Transverse Strength

The unidirectional composites were transversely tested in three-point bending at constant strain rate. All tests were performed at room temperature and showed perfect linear elastic behaviour up to failure. The results of maximum stress *versus* strain rate of the composites in three-point bending are presented in Figure 6. The error bars indicate the standard deviation of the experimental outcome.

As mentioned above, the mean strength measured at a strain rate of 1.7×10^{-4} s^{-1} was used as a reference to determine the critical value of the equivalent shear strain. For this purpose a micromechanical simulation of this experiment was performed, and stopped at a macroscopic stress level of 87 MPa, being the mean value of the experimentally determined strength. The distribution of the equivalent shear strain, at the macroscopic stress level of 87 MPa, is shown in Figure 7. The maximum value of the equivalent shear strain is 15.9% and is located in a small shear band close to the fibre-matrix interface, as indicated in Figure 7.

With this critical value obtained, it is now possible to predict the transverse strength at other strain rates. The predicted strain rate dependence of the trans-

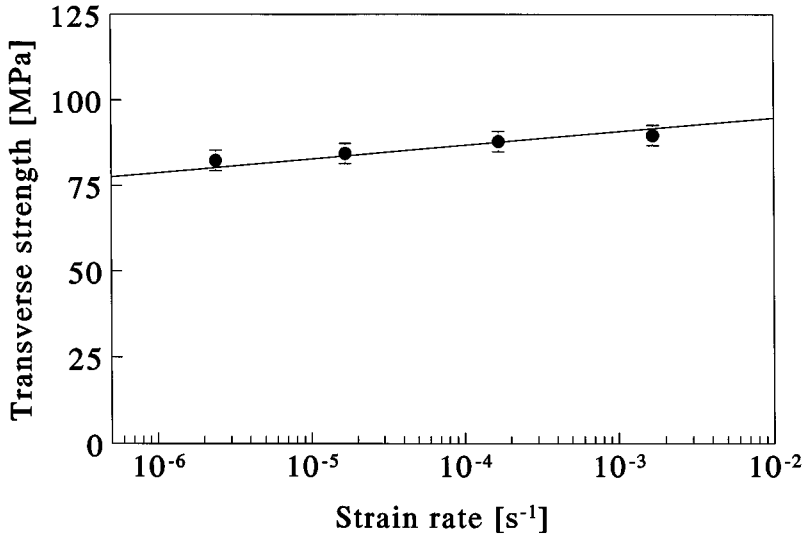

Figure 6. The transverse strength *versus* strain rate. The results of three-point bending on transversely loaded composites (markers) are compared with numerical simulations using the equivalent strain criterion (solid line).

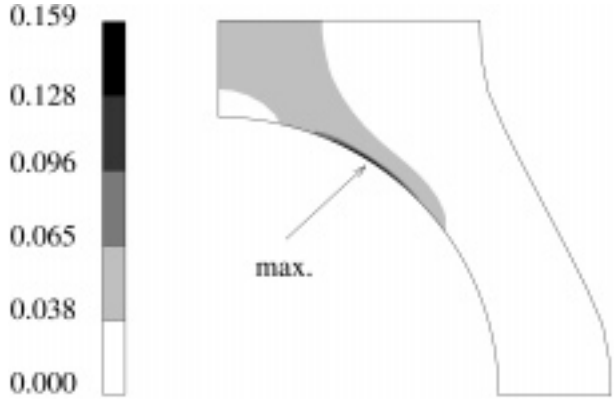

Figure 7. Contour plot of equivalent strain of the reference simulation at a global strain of 1.09% at which the experimentally obtained maximum strength occurred.

verse strength is represented by the solid line in Figure 6. This line was obtained by performing additional micromechanical simulations at strain rates of 10^{-3} and 10^{-5} s^{-1}. From Figure 6 it is clear that the experimental results are well represented by the micromechanical model employing a critical value for the equivalent shear strain $y_{eq} = 15.9\%$.

The stress-strain curves obtained from the micromechanical simulations are shown in Figure 8. At global strains below 0.6% the curves are identical for all strain rates due the initial rate-independent elastic behaviour of the matrix. The

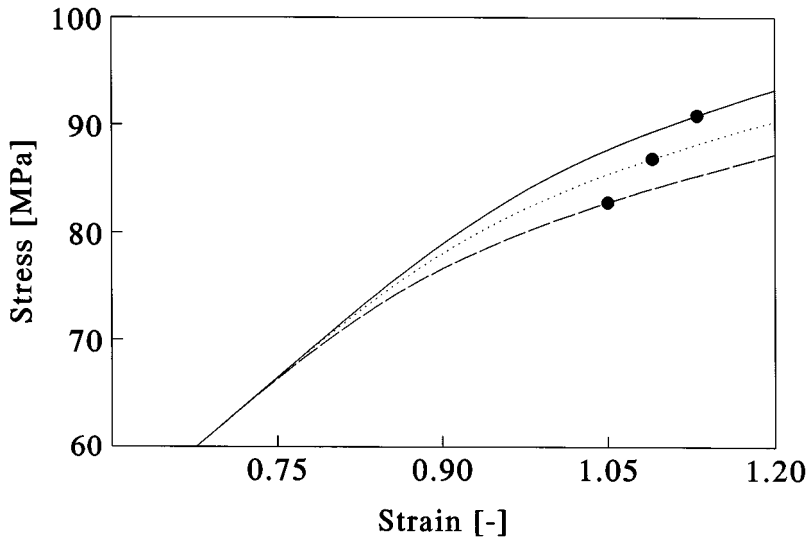

Figure 8. Numerical simulations of constant strain rate experiments at 10^{-3} (solid line), 10^{-4} (dotted line) and 10^{-5} s^{-1} (dashed line). The markers indicate the maximum transverse strength by using the equivalent strain criterion.

modulus, obtained from the curves in Figure 8 was 8890 MPa, which compares well to the experimentally obtained average value of 8760 MPa. In Figure 8 the predicted maximum strength employing the failure criterion is indicated by the markers. Please note that the increase of transverse strength with increasing strain rate also results in an increase in macroscopic strain-to-failure with increasing strain rate. This clearly indicates the inability of a *macroscopic* maximum strain criterion to predict time-variable failure phenomena.

5.2. Creep Lifetime

In this case the unidirectional composites were transversely loaded with a constant force in three-point bending. In all creep experiments the time needed to apply the constant engineering stress was negligible in comparison to the obtained creep time to failure. The applied stress was varied from 50 to 85 MPa. The results of the experiments are presented in Figure 9, where the arrow indicates a run-out.

Similar to the constant strain rate tests, the micromechanical model, in combination with the critical equivalent shear strain of 15.9%, was employed to predict the creep time to failure for the different applied engineering stresses. Micromechanical simulations of creep experiments at loads varying from 50 to 85 MPa were performed, and after each time-increment the maximum value of the equivalent shear strain was compared to the critical value. This procedure is demonstrated in Figure 10 where the evolution of the equivalent shear strain as a function of loading time is shown for a macroscopically applied stress of 75 MPa. The maximum value

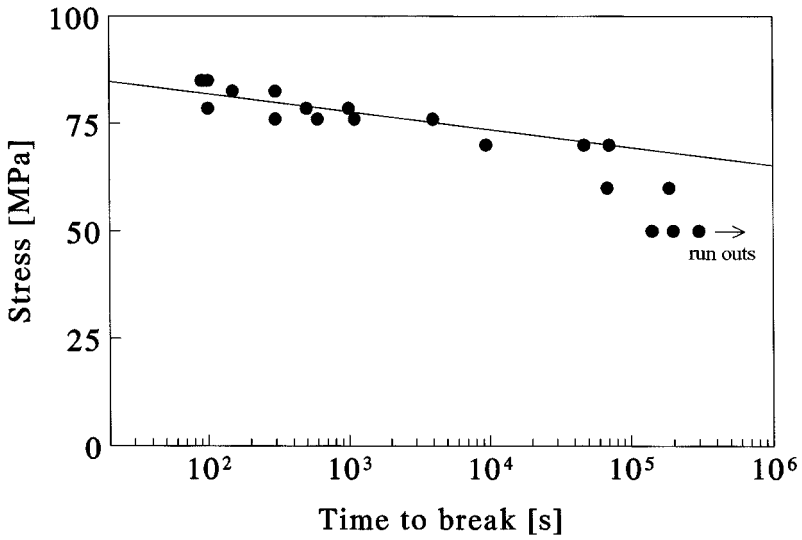

Figure 9. The applied stress *versus* time to break. The results of creep in three-point bending on transversely loaded unidirectional composites (markers) in comparison with simulations (solid line) using the equivalent strain criterion.

of γ_{eq} increases gradually and the critical value of 15.9% is reached after a loading time of 4100 s.

The results of the numerical simulations are compared to the experimental results in Figure 9, where the solid line represents the predicted time to failure *versus* the engineering stress using the equivalent shear strain criterion. It is clear that the micromechanical model in combination with this failure criterion is able to describe the experimentally observed time to fracture of the transversely loaded E-glass/epoxy composites.

6. Conclusions

In this study it is demonstrated that the modified Eyring equation can be satisfactorily used for the description of the yield behaviour of an epoxy system under multi-axial loading conditions. The various multi-axial experiments also showed that the epoxy system clearly exhibits a pressure-dependent yield behaviour.

By introduction of these parameters into the compressible Leonov model, numerical (FEM) simulations of the mechanical behaviour of the epoxy system could be performed. In combination with a representative volume element, based on a hexagonal stacking of the fibres, a micromechanical model was obtained. This model was subsequently employed to analyze time-dependent failure of unidirectional composites in transverse loading.

The critical value of the failure criterion, based on a local maximum of the equivalent shear strain, was determined by micromechanical evaluation of a refer-

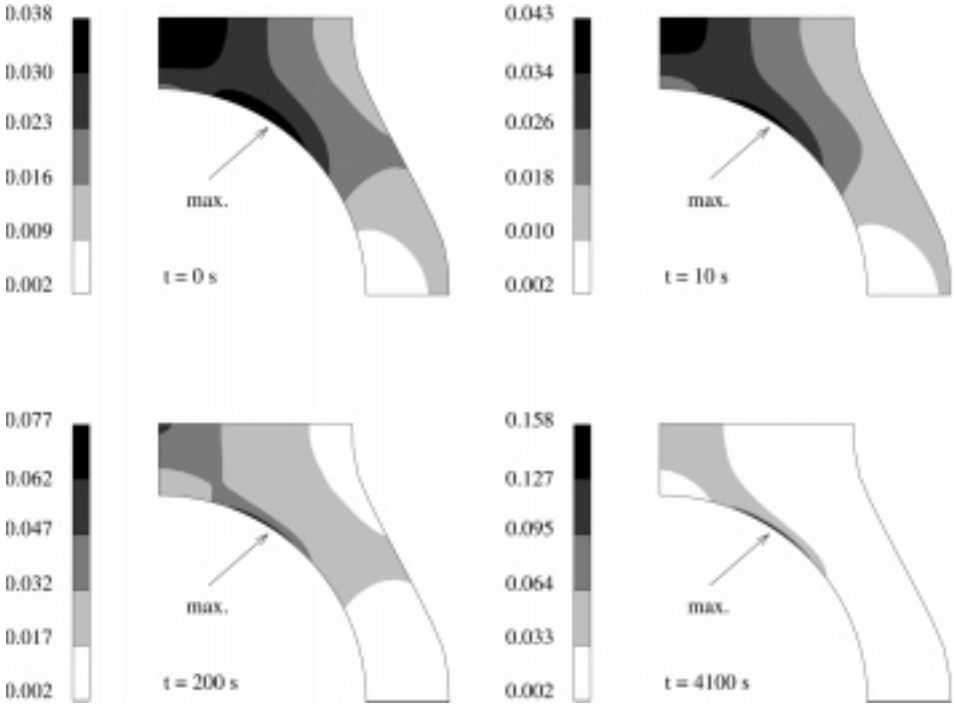

Figure 10. Contour plots of the evolution of the equivalent shear strain during a simulation of creep at an applied stress of 75 MPa. Contours are shown at creep times of 0, 10, 200 and 4100 s after load application.

ence experiment. The critical value of the equivalent shear strain obtained by this hybrid experimental/numerical technique was subsequently used for micromechanical simulations of rate-dependent transverse strength and creep time to failure. In both cases the numerical simulations were in good agreement with experimental observations.

References

Arruda, E.M. and Boyce, M.C., 'Evolution of plastic anisotropy in amorphous polymers during finite straining', *Internat. J. Plasticity* **9**, 1993, 697–720.

Asp, L., Berglund, L.A. and Gudmundson, P., 'Effects of composite-like stress-state on the fracture of epoxies', *Composites Sci. Technol.* **53**, 1995, 27–37.

Bird, R., Armstrong, R. and Hassager, O., *Dynamics of Polymer Liquids, Vol. 1: Fluid Mechanics*, John Wiley & Sons, New York, 1987.

Boyce, M.C., Parks, D.M. and Argon, A.S., 'Large inelastic deformation of glassy polymers. Part 1: Rate dependent constitutive model', *Mech. Mater.* **7**, 1988, 15–33.

Boyce, M.C., Arruda, E.M. and Jayachandran, R., 'The large strain compression, tension and simple shear of polycarbonate', *Polym. Engrg. Sci.* **32**, 1994, 716–725.

Brown, N., 'Yield behaviour of polymers', in *Failure of Plastics*, W. Brostow and R.D. Corneliussen (eds), Hanser Publishers, New York, 1986, 98–118.

De Kok, J.M.M., 'Deformation, yield and fracture of unidirectional composites in transverse loading', Ph.D. Thesis, Eindhoven University of Technology, Eindhoven, The Netherlands, 1995.

De Kok, J.M.M., Meijer, H.E.H. and Peijs, T., 'The influence of matrix plasticity on the failure strain of transversely loaded composite materials', in *Proceedings ICCM/9*, A. Miravete (ed.), Woodhead Publishing, Cambridge, 1993, 242–249.

Duckett, R.A., Goswami, B.C., Smith, L.S.A., Ward, I.M. and Zihlif, A.M., 'The yielding and crazing behaviour of polycarbonate in torsion under superposed hydrostatic pressure', *Brit. Polym. J.* **10**, 1978, 11–16.

Haward, R.N. and Young, R.J., *The Physics of Glassy Polymers*, 2nd edn., Chapman and Hall, London, 1997.

Haward, R.N., 'Strain hardening of thermoplastics', *Macromol.* **26**, 1993, 5860–5869.

Tervoort, T.A., Klompen, E.T.J. and Govaert, L.E., 'A multi-mode approach to finite, three-dimensional, nonlinear viscoelastic behavior of polymer glasses', *J. Rheol.* **40**, 1996, 779–797.

Tervoort, T.A., Smit, R.J.M., Brekelmans, W.A.M. and Govaert, L.E., 'A constitutive equation for the elasto-viscoplastic deformation of glassy polymers', *Mech. Time-Dependent Mater.* **1**, 1998, 269–291.

Tsai, S.W. and Hahn, H.T., *Introduction to Composite Materials*, Technomic Publishers, Basel, 1980.

Ward, I.M., 'Review: The yield behaviour of polymers', *J. Mater. Sci.* **6**, 1971, 1397–1417.

Ward, I.M., *Mechanical Properties of Solid Polymers*, 2nd edn., John Wiley & Sons, New York, 1983, 377–384.

Whitney, W. and Andrews, R.D., 'Yielding of glassy polymers: Volume effects', *J. Pol. Sci. C* **16**, 1967, 2981–2990.

Wu, P.D. and Van der Giessen, E., 'On improved network models for rubber elasticity and their applications to orientation hardening in glassy polymers', *J. Mech. Phys. Solids* **41**, 1993, 427–456.